Rev. Mexicana Astron. Astrof., **25**, 117-127 (1993)

NONLINEAR EVOLUTION OF ONE DIMENSIONAL COSMOLOGICAL INHOMOGENEITIES

V. Quilis, J.Mª. Ibáñez, and D. Sáez

Departamento de Física Teórica, Universidad de Valencia, Spain

Received 1993 February 26

RESUMEN

En este artículo, estudiamos la evolución no lineal de inhomogeneidades cosmológicas unidimensionales sin presión. Con el fín de resolver las ecuaciones en derivadas parciales que gobiernan esta evolución, hemos usado un algoritmo de *captura de choques de alta resolución*. Las condiciones iniciales se han tomado en el régimen lineal. El análisis se ha detenido en las proximidades de la formación de cáusticas. Nuestro código hidrodinámico ha generado satisfactoriamente la solución de Zel'dovich. Posibles mejoras y extensiones del trabajo son discutidas.

ABSTRACT

In this paper, we study the nonlinear evolution of one dimensional pressureless cosmological inhomogeneities. A *high-resolution shock-capturing algorithm* has been used in order to solve the partial differential equations governing this evolution numerically. Linear initial conditions have been considered. The analysis covers the epoch up to caustic formation. Our hydro-code has been tested in order to reproduce the Zel'dovich solution. Improvements and further extensions of this work are discussed.

Key words: **COSMOLOGY–THEORY — LARGE-SCALE STRUCTURE OF UNIVERSE**

1. INTRODUCTION

One of the main goals of Modern Cosmology is to explain structure formation in the Universe. It seems that such structure did grow from small amplitude primordial density fluctuations of the energy. These fluctuations would have arisen at the remote past and they would have grown due to gravitational instability. Although their origin has not been established definitely, it could be related to quantum fluctuations of the inflationary field (Kofman & Linde 1987). Such quantum fluctuations would have produced an initial Gaussian distribution (Bardeen, Steinhardt, & Turner 1983) of scalar adiabatic fluctuations, with a scale invariant spectrum.

Since the primordial fluctuations were originated with a small initial energy density contrast $\delta_i \ll 1$, their evolution can be studied by using perturbative methods (Brandenberger 1985; Mukhanov, Feldman, & Brandenberger 1992); in particular, the gauge invariant perturbation methods proposed by Bardeen (1980) and Ellis & Bruni (1989) deserve special attention. These methods give a good description of structure evolution up to the point where the density contrast δ becomes of the order of unity; then, a new epoch starts and is called *"the mildly nonlinear regime"*. The study of this period requires non perturbative methods. Most extensively used is the one based on a solution of the Newtonian equations describing the gravitational evolution of a pressureless fluid; this is the celebrated Zel'dovich approximation (Zel'dovich 1970). This solution is exact (Doroshkevich, Ryaben'kii, & Shandarin 1973; Shandarin & Zel'dovich 1989) in the one dimensional (1D) case. The three dimensional extension (3D) is only an approximation. Some authors have improved this 3D approximation (see Bertschinger 1991, and references therein). Other authors have found new 3D numerical solutions (Matarrese, Pantano, & Sáez 1993). Unfortunately, the above methods and solutions are only valid up to *caustic formation*. The contrast δ tends to infinity, in a finite time t_c, in the caustics, its value being about unity outside them. The very steep gradients developed near caustics, in times close to t_c, suggest the use of *Godunov type methods* (Godunov 1959), which were designed for treating more problematic situations with discontinuities.

In the case of a *pressureless fluid, which evolves under the action of purely gravitational forces, from general cosmological initial conditions*, caustic formation is

unavoidable. In order to prevent these divergencies and to be able to go beyond the mildly nonlinear regime, towards the *strongly nonlinear regime*, which dominates inside structures such as galaxy clusters, only two alternatives are possible: either matter is not described as a fluid, or non gravitational forces must be introduced. These alternatives have motivated several approaches and numerical techniques which can be classified in two types, basically: P (particle) and F (fluid).

In the *P approach*, matter is not a fluid, but a discrete system of particles, and forces are purely gravitational. The popular *N-body* simulations, in which a set of N particles defines a self-gravitating system, belong to this type of approaches.

In the *F approach*, matter is a fluid, but nongravitational forces prevent the *shell crossing*, which is responsible for caustic formation. Among the various models within the F approaches, the so-called *Adhesion model* (Gurbatov, Saichev, & Shandarin 1989) stands out: a numerical artificial viscosity prevents caustic formation. These techniques have been applied to several physical problems. Von Neumann & Richtmyer (1950) were the first to use them in hydrodynamics. Models which make use of artificial viscosity have been successful in the treatment of shocks and discontinuities, although as Noh (1987) showed, they can be a source of intrinsic errors and, as Noh suggested, they can be improved at the cost of more experimentation on the free parameters. Another F approach is the *"Frozen flow model"* recently proposed by Matarrese et al. (1992), in which the particle velocities in the nonlinear regime are identified with the linear ones. These velocities could only be produced by fictitious nongravitational forces, which prevent caustic formation.

The present work is part of a research project, in which we try to build up a numerical code describing the matter as a fluid with pressure. Pressure gradients would be the forces preventing caustic formation. Pressure could produce shocks and smoothing of gradients (preventing or delaying divergencies of δ). This smoothing could facilitate the application of any numerical method, and the possible presence of shocks strongly suggests the use of techniques such as *Godunov-type methods*, which were especially prepared to study the evolution of these discontinuities. Due to these reasons, the partial differential equations which describe the evolution of the fluid (Peebles 1980) would be numerically solved using *Godunov type techniques* (Godunov 1959) or more precisely *modern high-resolution shock-capturing methods*.

Although pressure would play an important role in the code we are trying to elaborate in this paper, we are going to assume that pressure is zero. There are two main reasons for this assumption: (1) The Zel'dovich 1D exact solution can be used as a test, (2) the application of Godunov-type methods is more involved for vanishing pressure (divergencies of δ) and, consequently, if any of these methods work well in the pressureless case $P = 0$, it should not fail for $P \neq 0$ (in spite of the possible presence of shocks).

Godunov-type methods have undergone an important development in the eighties. They have been applied in problems of Computational Fluid Dynamics (aerodynamics, etc.) and in Astrophysics (see, for example Fryxell, Müller, & Arnett 1990). These methods have been extended to relativistic hydrodynamics by the Valencia group (Martí et al. 1990; Martí, Ibáñez, & Miralles 1990; Martí 1991; Font et al. 1993). Their main features are: *i*) They are highly accurate in the smooth regions of the flow, and *ii*) they give high resolution in the regions of discontinuities, avoiding the use of artificial viscosity. The original Godunov method (1959) is first order accurate (see § 2.3). This method was used by Doroshkevich & Shandarin (1973) to study nonlinear disk-shaped concentrations of matter (development of the pancake theory). In this paper, we use a second order accurate modern high-resolution shock-capturing algorithm (see § 2.3).

In the case of a pressureless fluid, there are no nongravitational forces able to avoid caustic formation; hence, regions with large values of δ and their gradients will appear. In these regions, the evolution equations have been integrated up to the point at which large values of δ are very high, thanks to the special features of Godunov-type methods combined with rezoning techniques.

Henceforth, t is the cosmological time, t_0 is the age of the universe, $a(t)$ is the scale factor of a flat Friedman-Robertson-Walker background. $\dot{X}$ stands for the derivative of function X with respect to the cosmological time. The present value $H(t_0)$ of the function $H = \dot{a}/a$ is the Hubble constant; its value in units of 100 km s^{-1} Mpc^{-1} is h. ρ_B is the background density, ρ is the density of the cosmological fluid, $\delta = (\rho - \rho_B)/\rho_B$ is the density contrast and, finally, c is the speed of light.

This paper is structured as follows: in § 2, a brief description of the Godunov-type methods is shown, and a numerical code designed to study the evolution of 1D inhomogeneities is presented. In § 3 some exact solutions are described. The numerical code is tested in § 4, where the exact solutions are numerically recovered. The main conclusions and our projects are presented in § 5.

2. GODUNOV-TYPE METHODS

2.1. Definitions

A system of equations is called a *hyperbolic system of conservation laws* in the sense of Lax (1973) —in one dimension— if it can be written in the form:

$$\frac{\partial \mathbf{u}}{\partial t} + \frac{\partial \mathbf{f(u)}}{\partial x} = 0, \quad (1)$$

where **u** is the N-dimensional vector of unknowns and **f(u)** is a vector of functions of dimension N; these functions are called *fluxes*. The above system is called *strictly hyperbolic* if the Jacobian of the matrix

$$A = \frac{\partial \mathbf{f(u)}}{\partial \mathbf{u}}$$

has N eigenvalues $\lambda_\alpha (\alpha = 1,...N)$ real and different, and the set of eigenvectors is complete in $\Re^N$.

For the sake of simplicity let us consider the scalar case (N = 1). It is known as a *Riemann problem*, the initial value problem for the system (1) with the discontinuous data:

$$u(x,0) = \begin{cases} u_L & \text{if} \quad x < x_{dis} \\ u_R & \text{if} \quad x > x_{dis} \end{cases} ,$$

where u_R and u_L are, respectively, the values of u at the right and at the left side of the discontinuity (x_{dis}).

Since the initial conditions are discontinuous, we are concerned with weak solutions, i. e., solutions in the sense of the distribution theory; in general, the weak solution of a Riemann problem is not unique. For scalar equations, it has been proved (Oleinik 1963; Lax 1973) that a weak solution is the relevant physical one if the following conditions are satisfied: the *Rankine-Hugoniot relations*

$$f(u_R) - f(u_L) = s(u_R - u_L) , \quad (2)$$

and the *entropy conditions*

$$\frac{f(u) - f(u_L)}{u - u_L} \geq s \geq \frac{f(u) - f(u_R)}{u - u_R} ; \quad (3)$$

where s is the propagation speed of the discontinuity (Martí 1991). A numerical method must be designed in such a way that it generates the physically relevant weak solution. The discontinuities are classified in *shocks*, if the above inequalities are strict, and *contact discontinuities* if the equalities hold identically.

The extension to systems of equations of a high-resolution shock-capturing scheme is carried out, in a natural way, by using the *local characteristic approach* (see, i.e., Martí 1991, and references therein).

2.2. *The Evolution Equations of Cosmological Inhomogeneities in Conservative Form*

We are going to show that the evolution equations of cosmological inhomogeneities can be written in the form:

$$\frac{\partial \mathbf{u}}{\partial t} + \frac{\partial \mathbf{f(u)}}{\partial x} = \mathbf{s(u)} ; \quad (4)$$

that is, as a one dimensional hyperbolic system of conservation laws with sources **s(u)**. The treatment of the sources requires specific techniques, which depend on the desired accuracy and the complexity of these terms. In our case, they are included in the temporal advance algorithm [see next subsection, equation (18)].

The evolution equations for a cosmological inhomogeneity evolving in a Robertson-Walker background, in the absence of pressure, and under the action of purely gravitational forces, are the following (Peebles 1980):

$$\frac{\partial \delta}{\partial t} + \frac{1}{a}\nabla \cdot (1+\delta)\vec{v} = 0 , \quad (5)$$

$$\frac{\partial \vec{v}}{\partial t} + \frac{1}{a}(\vec{v} \cdot \nabla)\vec{v} + H\vec{v} = -\frac{1}{a}\nabla\phi , \quad (6)$$

and

$$\nabla^2\phi = \frac{3}{2}H^2 a^2 \delta ; \quad (7)$$

where $\vec{x}$, $\vec{v} = a(t)\, d\vec{x}/dt$ and $\phi(t,\vec{x})$ are, respectively, the Eulerian coordinates, the peculiar velocity and the peculiar Newtonian gravitational potential.

The Newtonian description given by equations (5)–(7) can suffice, instead of a relativistic one (Peebles 1980), if a set of conditions are satisfied. We can distinguish two cases: a) the background is flat (as in this paper); in this case the use of equations (5)–(7) demands that the peculiar velocities be lower than the speed of light ($v \ll c$), and b) the background is either open or closed; now, in addition to the above restriction on the velocities, the inhomogeneity size must be smaller than the causal horizon size (negligible background curvature). Condition b) would be also necessary in the flat case, if one considers that the total velocities (not the peculiar ones) must be lower than c.

In all our applications we have verified that the above conditions about velocities and sizes are satisfied. Finally, very close to the caustics, δ diverges and, consequently, it reaches arbitrarily large values as the time becomes close enough to t_c. Hence, the use of General Relativity would become necessary; however, in our calculations, δ takes values around 10^3, which implies $\rho \sim 10^{-26}$ gr cm^{-3}.

In 1D cases, equations (5) and (6) can be easily written as follows:

$$\frac{\partial \delta}{\partial t} + \frac{\partial}{\partial x}[(\delta + 1)\frac{v}{a}] = 0 \qquad (8)$$

and

$$\frac{\partial v}{\partial t} + \frac{\partial}{\partial x}[\frac{v^2}{2a}] = -\frac{1}{a}\frac{\partial \phi}{\partial x} - vH \ . \qquad (9)$$

These equations have the form (4) if the following variables, fluxes, and sources are defined as:

$$\mathbf{u} = [\delta, v] \ , \qquad (10)$$

$$\mathbf{f(u)} = [\frac{v(\delta + 1)}{a}, \frac{v^2}{2a}] \ , \qquad (11)$$

and

$$\mathbf{s(u)} = [0, -\frac{1}{a}\frac{\partial}{\partial x}\phi - Hv] \ . \qquad (12)$$

Furthermore, the 1D version of Poisson's equation is:

$$\frac{\partial}{\partial x}[\frac{\partial}{\partial x}\phi] = \frac{3}{2}H^2 a^2 \delta \ . \qquad (13)$$

Equations (8) and (9) are not a strictly hyperbolic system because the eigenvalues of the matrix $A = \partial f(u)/\partial u$ are not distinct; however, each of these equations is a scalar hyperbolic equation. In the absence of source terms, equation (9) is the well-known Burgers equation. The source terms couple both scalar equations. In practice, we have proceeded as follows: first, equation (9) has been solved in order to compute v and, afterwards, v has been used as input in equation (8) to compute δ.

Poisson's equation (13) is elliptic. It has been only used to compute the source term $\partial\phi/\partial x$ which appears in equation (9). At each instant, equation (13) is integrated as a first order ordinary differential equation in the variable $\partial\phi/\partial x$.

2.3. *Some Details about our Code*

In this paper we have used a *modern high-resolution shock-capturing* method which is, nowadays, one of the generalizations of the original Godunov's idea. More precisely, we have applied a version of the MUSCL's algorithm (Monotonic Upstream Schemes for Conservation Laws), derived by Van Leer (1979), together with other ingredients — approximate Riemann's solver, semiadapted spatial grid, a specific time step,...— that we are going to describe in a summarized way. The details can be found in Martí (1991) and references cited therein.

The main components of our MUSCL algorithm are the following:

1. At each time step $t = t^n$, the data u_j^n are the *cell-averaged* of the variables $u(x,t)$

$$\mathbf{u}_j^n = \frac{1}{\Delta x_j}\int_{x_{j-1/2}}^{x_{j+1/2}} \mathbf{u}(\mathrm{x}, \mathrm{t}^n)\mathrm{dx} \ ; \qquad (14)$$

where $j - 1/2$ and $j + 1/2$ stand for the lower and upper (or left and right) interfaces, respectively, of the numerical cell j. These cell-average quantities are evolved in time (see below).

2. *Reconstruction procedure* from the cell-averaged quantities u_j^n. With this aim we have carried out a linear reconstruction which preserves monotonicity. In particular, we have made use of the *minmod* function as a slope limiter. The *minmod* function chooses the lower slope from the other two defined by quantities u_{j-1}^n and u_j^n on one side, and u_j^n and u_{j+1}^n on the other side. Hence, at each time level there exists a coupling among three consecutive cells, $j - 1$, $j, j + 1$ allowing to establish the corresponding Riemann problems at the interfaces $j - 1/2$ and $j + 1/2$, respectively.

3. Computation of the *numerical fluxes* at interfaces. Component i^{th} of the numerical flux is calculated according to Roe's prescription (Roe 1981):

$$\hat{f}^{(i)}_{j+\frac{1}{2}} = \frac{1}{2}\Big(f^{(i)}(\mathbf{u}^L_{j+\frac{1}{2}}) + f^{(i)}(\mathbf{u}^R_{j+\frac{1}{2}}) - \sum_{\alpha=1}^{2} |\tilde{\lambda}_\alpha| \Delta\tilde{\omega}_\alpha \tilde{R}^{(i)}_\alpha\Big) \ . \qquad (15)$$

Where L and R stand for the states to the left and right of a given interface ($j + \frac{1}{2}$). $\tilde{\lambda}_\alpha$ and $\tilde{R}^{(i)}_\alpha$ ($\alpha = 1,2$) are, respectively, the eigenvalues (that is, the *characteristic velocities*) and the i^{th} component of the α-right eigenvector) of the Jacobian matrix:

$$\mathbf{A}_{j+\frac{1}{2}} = \Big(\frac{\partial \mathbf{f(u)}}{\partial \mathbf{u}}\Big)_{\mathbf{u}=(\mathbf{u}^L_{j+\frac{1}{2}} + \mathbf{u}^R_{j+\frac{1}{2}})/2} \ . \qquad (16)$$

And quantities $\Delta\tilde{\omega}_\alpha$ —the jumps in the local characteristic variables through each interface— are obtained from the following relation

$$u^{(i)}_R - u^{(i)}_L = \sum_{\alpha=1}^{2} \Delta\tilde{\omega}_\alpha \tilde{R}^{(i)}_\alpha \ . \qquad (17)$$

$\tilde{\lambda}_\alpha$, $\tilde{R}_\alpha^{(i)}$ and $\Delta\tilde{\omega}_\alpha$, as functions of $\mathbf{u}$, are calculated at each interface and, thus, they depend on the particular values $\mathbf{u}_L$ and $\mathbf{u}_R$.

4. *Advancing in time.* Once the numerical fluxes, $\hat{f}$, are known (they carry the complete information of the system) the evolution of quantities $\mathbf{u}_j$ are governed by

$$\frac{d\mathbf{u}_j(t)}{dt} = -\frac{\hat{\mathbf{f}}_{j+\frac{1}{2}} - \hat{\mathbf{f}}_{j-\frac{1}{2}}}{\Delta x} + \mathbf{s}_j \ . \tag{18}$$

The above equation can be solved by standard ordinary differential equation solvers. Our MUSCL version uses a "predictor-corrector" method with an appropriate time step (see below).

It can be shown that the "minmod" reconstruction, Roe's prescription for evaluating the numerical fluxes, and the "predictor-corrector" method for solving (18), set out a global second order accurate algorithm.

To end this section, let us notice some features of our computational grid. We have said that our algorithm is second order accurate globally, i.e., the *local error of truncation* is of order $O[(\Delta x)^2]+O[(\Delta t)^2]$. Refining the grid accelerates the convergence. The choice of the time step is crucial for the stability of the scheme.

In the neighborhood of the caustics, we have proceeded to refine the spatial grid in order to get an adequate resolution.

The time step used for solving equation (18) has a value which varies according to some criteria. When the inhomogeneity evolves and enters into the very fast nonlinear regime, the time step must be lower than the one corresponding to the slow linear regime. In order to keep into account this feature, we have implemented the following criterion: first, we estimate the time step between time levels t^n and t^{n+1}, $\Delta t^{n+1/2}$, according to $\Delta t^{n+1/2} = t^n/10^3$. Second, we evaluate the relative variation

$$\Delta\mathbf{u}_j = \frac{|\mathbf{u}_j^{n+1} - \mathbf{u}_j^n|}{|\mathbf{u}_j^n|} \ . \tag{19}$$

If $\Delta\mathbf{u}_j$ satisfies the condition $\Delta\mathbf{u}_j \leq 10^{-2}$ for all numerical cells and all components of $\mathbf{u}$, then, the estimated time step, $\Delta t^{n+1/2}$, is accepted. Otherwise, this time step is divided by a factor of two and the process is repeated until the tolerance is fulfilled. By construction, this procedure takes into account the rapid variations of variables δ and v in the nonlinear regime. We have verified that $\Delta t^{n+1/2}$ is always lower than the so-called *Courant time* in order to guarantee the stability of the scheme (Courant, Friedrichs, & Lewy 1928).

3. THE ZEL'DOVICH SOLUTION

In the 1D case, Zel'dovich solution satisfies exactly the system (5)–(7). A brief description of this solution is now presented. Its applications are studied in the next section.

In order to get the Zel'dovich 1D solution, it is assumed that *the flow is potential*, it means that the velocity dx/da derives from a velocity potential $\phi_z(q)$;

$$\frac{dx}{da} = -\nabla_q\phi_z(q) \ . \tag{20}$$

Where q is the Lagrangian coordinate which coincides with the Eulerian coordinate x at the initial time t_i. A simple integration of equation (20) leads to the following relation:

$$x = q - [a(t) - a(t_i)]\nabla_q\phi_z(q) \ . \tag{21}$$

Zel'dovich solution can be easily derived by substituting condition (20) into the system (5)–(7). This solution is completely defined by the function $\phi_z(q)$, its explicit form is now presented for the velocity potential

$$\phi_z(q) = -A\cos(kq) \ , \tag{22}$$

A and k being free parameters. k defines the spatial size of the perturbation and A its amplitude.

The peculiar Zel'dovich velocity is

$$v(x,t) = -\dot{a}(t)a(t)Ak\,sin(kq) \ , \tag{23}$$

and the gravitational peculiar potential (Doroshkevich, Ryaben'kii, & Shandarin 1973) is

$$\phi_g(x,t) = -\frac{3}{2}a\dot{a}^2[\phi_z(q) + \frac{(x-q)^2}{2(a(t)-a(t_i))}] \ ; \tag{24}$$

where the second term inside the bracket tends to zero as the time tends to its initial value t_i. Putting this potential into equation (7), the function $\delta(x,t)$ is easily obtained; in particular, the initial profile of the density contrast $\delta_i = \delta(x,t_i)$ is found.

Additionally, introducing the peculiar velocity (23) into equation (5), and integrating the resulting equation, the following relation is formally found

$$\delta(x,t) = \frac{\delta(x,t_i)+1}{1-(a(t)-a(t_i))Ak^2\cos(kq)} - 1 \ , \tag{25}$$

in which, the initial δ profile is not free (see above).

At $x = 0$ ($q = 0$), the contrast (25) diverges at the time t_c, which satisfies the following equation:

$$a(t_c) - a(t_i) = A^{-1}k^{-2} \quad . \tag{26}$$

Zel'dovich solution coincides with the *linear one* for small values of δ; hence, in the linear regime, the initial profile, δ_i, corresponding to the velocity potential (22) is $\delta_i = Ak^2 \cos(kq)$. Out of the linear regime, δ_i has to be computed by using equations (7) and (24), as it has been explained above.

To end this section, let us present several considerations, which are important in order to describe the second test of the next section. If the initial arbitrary contrast δ_i evolves according to the velocity field (23), the resulting contrast $\delta(x,t)$ is given by equation (25). In order to prove it, just substitute (23) into the continuity equation and check that the resulting equation has solution (25). It is worthwhile to point out that, for a free δ_i, equations (23) and (25) define a solution of the continuity equation, which does not coincide, in general, with the Zel'dovich solution of the system (5)–(7) (which corresponds to a well defined profile δ_i, as discussed above). This means that, for a free δ_i, the velocities (23) cannot be produced by the gravitational forces created by the contrast (25); however, other forces producing the velocities (23) would transform the initial profile δ_i in agreement with (25).

4. GENERAL RESULTS AND DISCUSSION

In this section we show two cosmological tests which our code has overcome: 1) Zel'dovich 1D solution (§ 4.1). 2) Evolution of discontinuous initial profile of density contrast (§ 4.2).

In both cases, the analytical solutions are compared with the corresponding numerical ones. The initial data, that is, the δ and v profiles, are the ones given by the analytical solution particularized at the initial time t_i.

In all figures displayed here we have used circles for denoting the numerical values and continuous lines for the exact solutions.

4.1. A Test Based on Zel'dovich 1D Solution

We have evolved initial data given at time t_i, corresponding to a redshift $z_i = 50$, at which, the inhomogeneities evolve into the linear regime.

We have considered two different inhomogeneities, called Z1 and Z2, corresponding to a Zel'dovich potential of the form (22) (see §3). These inhomogeneities are characterized by parameters A and k. Table 1 displays the values of these parameters as well as the initial contrast δ_i and the time of caustic formation t_c. Inhomogeneity Z1 is larger than Z2 and, hence, Z2 reaches the nonlinear regime earlier than Z1. Caustics appear, in the case of Z2 (Z1), before (after) present time $t_c < t_0 (t_c > t_0)$. Due to the fact that the inhomogeneities are 1D and the potentials have been chosen periodic, we can interpret these structures as walls centered at the points $q_n = 2\pi n/k$, with n integer. As time goes on, these walls become increasingly narrower and denser. We have shown, in our figures, only the wall centered at $q = x = 0$.

TABLE 1

PARAMETERS FOR THE 1D ZEL'DOVICH SOLUTION[a]

Case	A(h Mpc^{-1})	k	δ_i	t_c
Z1	9.1×10^{-3}	0.35	0.001	$5t_0$
Z2	9.1×10^{-4}	3.5	0.001	$0.2t_0$

[a] See text for details about entries.

Figure 1 shows the evolution of the Z1 inhomogeneity. The two upper curves correspond to the density contrast profile δ (upper left) and the peculiar velocity profile v (upper right) as functions of the adimensional Eulerian coordinate x. The scale factor is given in units of 21.96 h^{-1} Mpc, and the distance to the inhomogeneity center, in units of h^{-1} Mpc, is $d = xa$. These two profiles correspond to the instant $t/t_c = 0.964$, being the maximum —in space— of $\delta \sim 40$ and the maximum of $v \sim 0.15$c. The couple of curves in the middle and the lower parts of Figure 1 show the same quantities but at different times, $t/t_c = 0.992$ and $t/t_c = 0.998$, respectively, being the corresponding extrema: maximum of $\delta \sim 200$ (~ 800) and maximum of $v \sim 0.125$ (~ 0.125) for the curves displayed at the middle (lower) part of Figure 1. The main conclusion from this figure is that our numerical results and the exact ones agree —both for the contrast density and for the peculiar velocity— with a relative error between 10^{-5} and 10^{-4}, with the exception of the central point $x = 0$, where the difficulties associated with the existence of very steep gradients become more severe. At this point the relative error is between 10^{-2} and 10^{-1}.

In order to treat numerically the evolution in the strongly nonlinear regime, we have refined the spatial grid in the neighborhood of $x = 0$. The initial number of cells, 250, is kept fixed while δ is lower than ~ 10, otherwise a rezoning is carried out in such a way that the final number of cells is 1290 when is $\delta \sim 10^3$. From the upper left curve we can conclude that the thickness of the resulting wall amounts to $\sim 10^2$ Mpc, being the diameter of the horizon $\sim 10^4$ Mpc, at the time $t \sim t_c \sim 5t_0$. As it can be seen from the upper right curve of Figure 1, peculiar velocities are always lower than 0.15c,

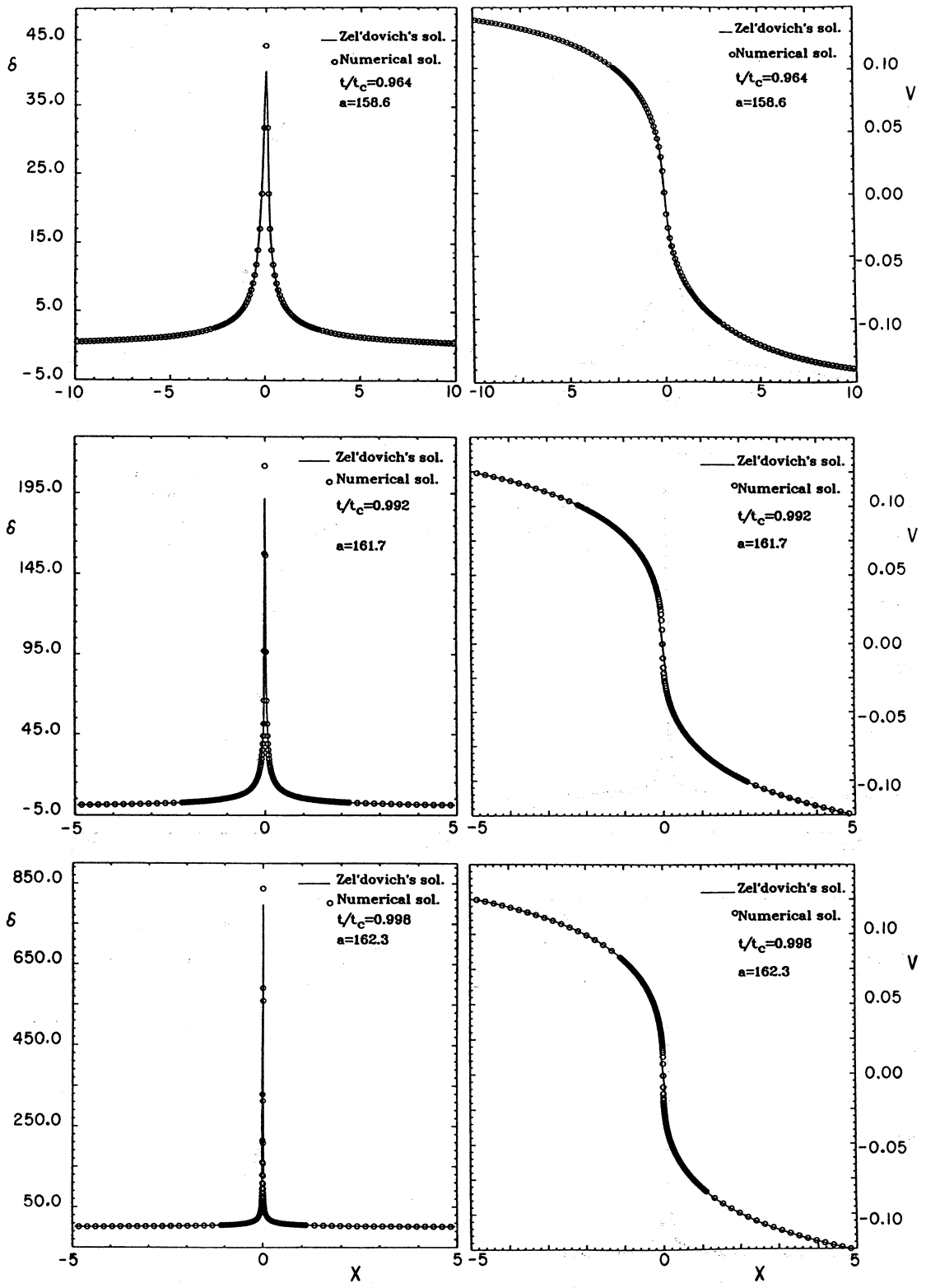

Fig. 1. Density contrast (left) and peculiar velocity (right) as functions of the adimensional Eulerian coordinate x for the inhomogeneity Z1. Circles correspond to the numerical values and continuous line to the Zel'dovich solution. Time is given in units of t_c and the scale factor in units of 21.96 h^{-1} Mpc.

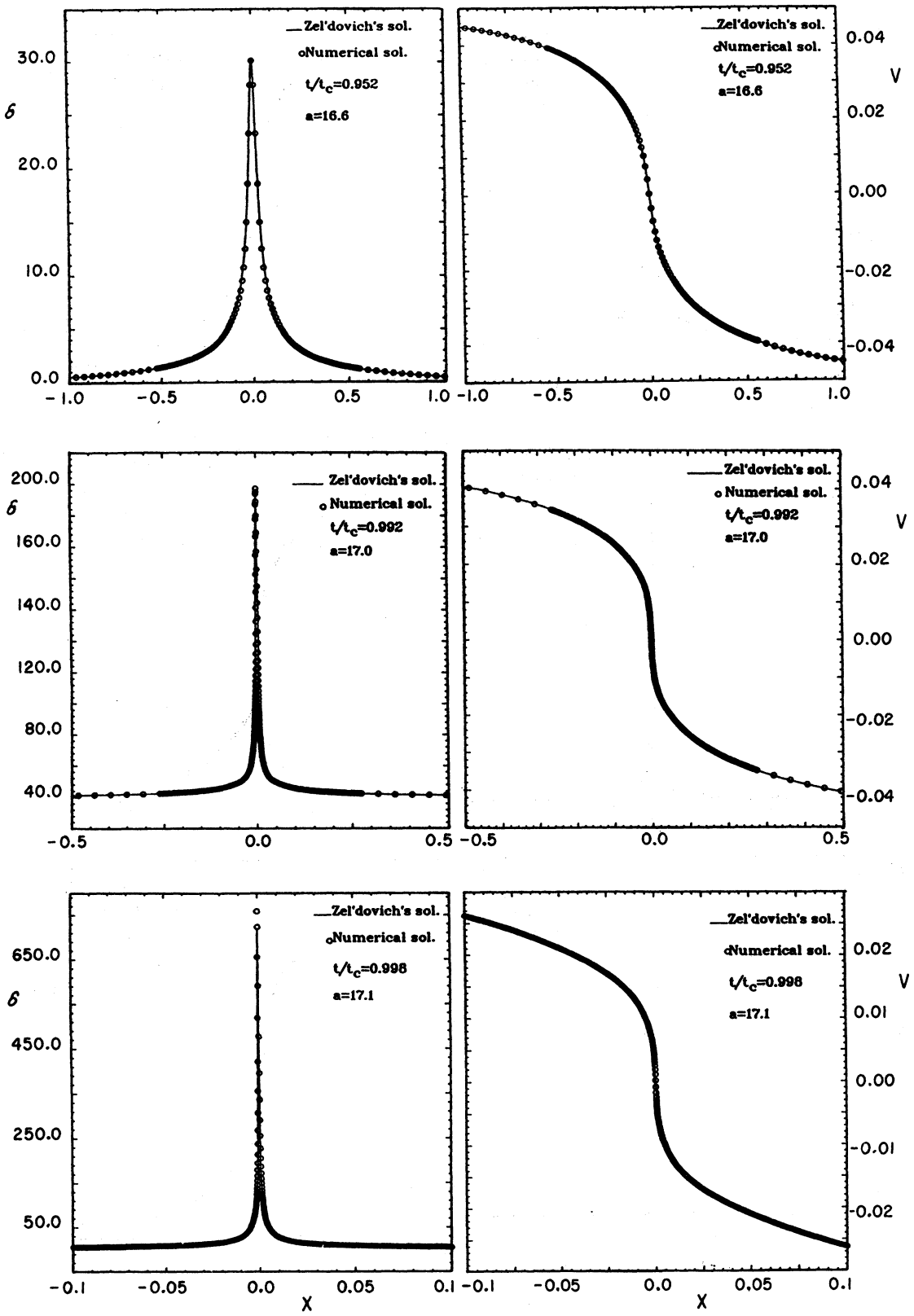

Fig. 2. Same as Figure 1 for the inhomogeneity Z2.

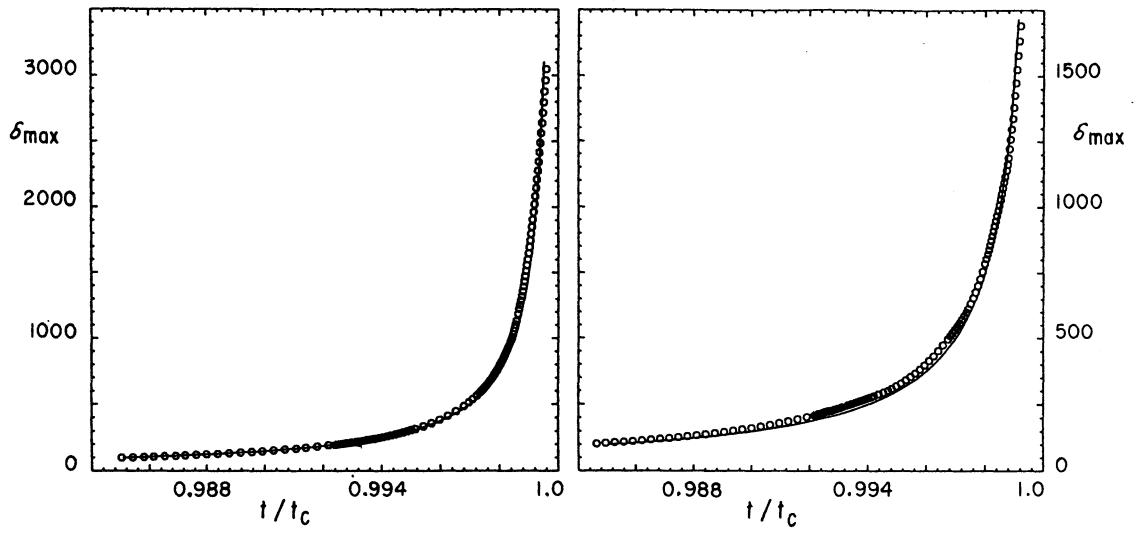

Fig. 3. Maximum value of the density contrast as a function of time (in units of t_c). The curve on the right (left) correspond to inhomogeneity Z1 (Z2).

hence, we can conclude that the system is non-relativistic and the Newtonian approach defined by equations (5)–(7) might be sufficient (see § 3). The same conclusions are found from the other curves of Figure 1.

The evolution of inhomogeneity Z2 is described in Figure 2. This figure is analogous to Figure 1, and we will not comment on it. As in the case of Z1, the inhomogeneity Z2 does not require a relativistic treatment. But, unlike the Z1 case, Z2 requires a more refined mesh. We have used 250 numerical cells with $\delta \sim 1$ or lower, and the mesh has been refined to a total of 5265 points in order to resolve a density contrast of $\delta \sim 3000$. These grids allow to overcome the numerical problems associated with the huge spatial and temporal gradients developed by inhomogeneity Z2, which correspond to a very thin nonlinear wall.

Finally, Figure 3 shows the evolution of the maximum —in space— of the density contrast δ_{max}. The curve on the right of Figure 3 corresponds to inhomogeneity Z1 and the one on the left to Z2. It can be seen from it, according to the predictions of Zel'dovich 1D solution, that δ_{max} diverges as time (in units of t_c) tends to unity. The most important feature of Figure 3 is the good agreement between the numerical and exact solutions, in both cases, and including the region where δ_{max} rapidly increases.

4.2. A Test Based on the Equation of Continuity

As we have discussed in section § 3, an arbitrary initial profile of the density contrast $\delta_i(x)$, evolving with the peculiar velocity given by equation (23), varies with time according to equation (25). Equation (25) is an exact solution of the continuity equation, which is to be compared with the numerical solution corresponding to the same initial values and the same peculiar velocities (23).

In all the cases considered in this subsection, the initial redshift is $z_i = 500$ and the constants of the equation (23) take the values $A = 1.45 \times 10^{-3}$ h Mpc^{-1} and $k = 9.8 \times 10^{-2}$. Caustic formation appears, in all cases, at $t_c = 13 t_0$.

We have studied the evolution of the following three different initial profiles δ_i: 1) Case C1: $\delta_i = 1$ if $x \in [-0.5,0.5]$ and $\delta_i = 0$; 2) Case C2: $\delta_i = 4$ if $x \in [-0.25,0.25]$ and $\delta_i = 0$; 3) Case C3: $\delta_i = 10$ if $x \in [-0.1,0.1]$ and $\delta_i = 0$. These three "step-like" discontinuous profiles have been chosen with the only aim of checking the capacity of our numerical code to treat discontinuous initial data. They do not represent any real cosmological structure at all.

Figure 4 shows the density contrast profiles as functions of x at the instant $t \sim 0.15 t_c$. The upper left curve corresponds to C1, the upper right one corresponds to C2 and the lower one to C3. It is obvious that the agreement between the exact solution and the numerical one is excellent. That gives us confidence on the feasibility of our code for treating discontinuous initial data. The grid used in the three cases has 480 points and it has not been refined. A rezoning could be necessary at a late epoch, in particular, close to the critical time.

5. CONCLUSIONS AND PERSPECTIVES

A numerical code based on the MUSCL algorithm has been built up. Several severe tests have been overcome by our code. This code combines the following ingredients: a linear reconstruc-

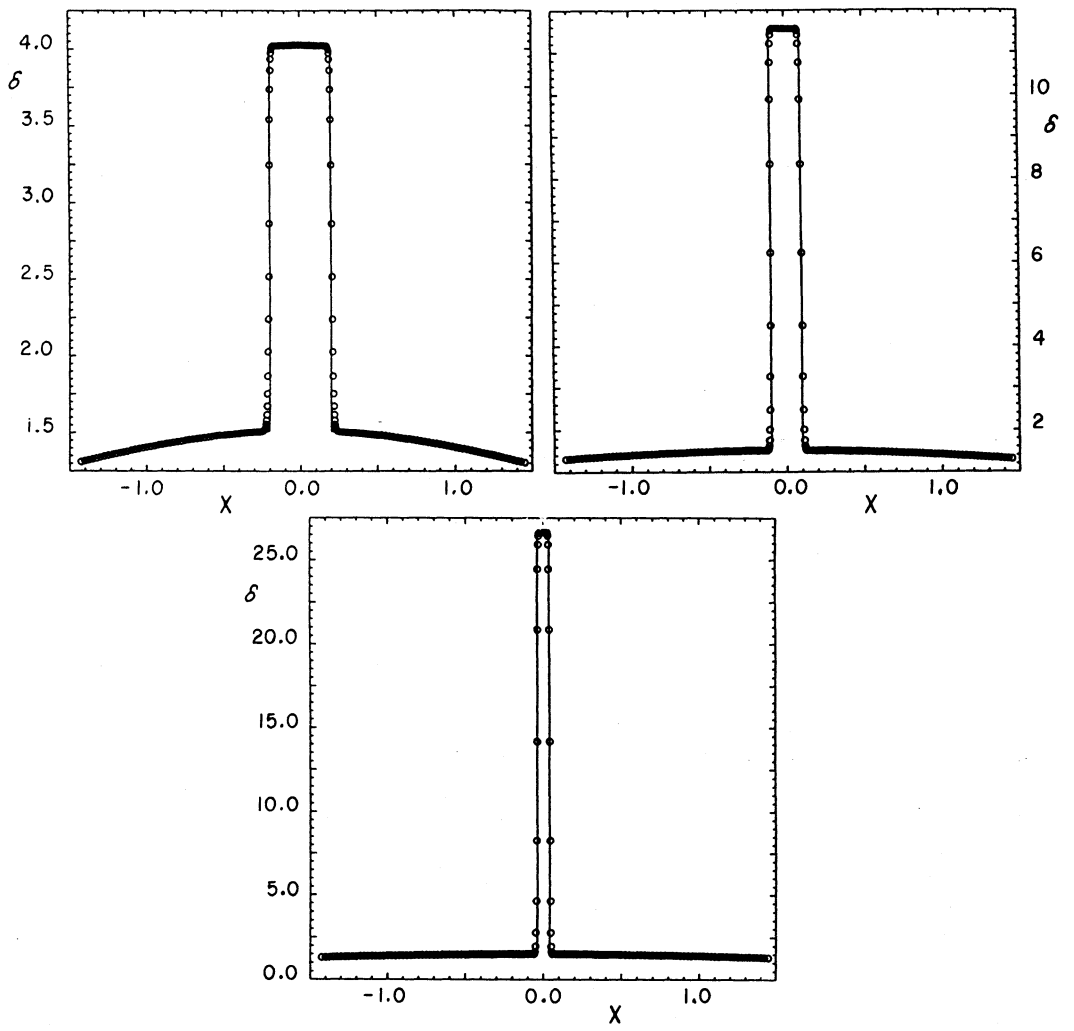

Fig. 4. Density contrast δ as a function of the adimensional Eulerian coordinate x at the time $t/t_c \sim 0.15$. Cases C1, C2 and C3 correspond to the upper left, upper right and lower curves (see text for details). In all cases $a = 784.3$, in units of 21.96 h^{-1} Mpc.

tion, Roe's prescription for evaluating the numerical fluxes and a predictor-corrector method for advancing in time. Our code is globally second order accurate. It has been applied to the study of how one dimensional pressureless cosmological inhomogeneities evolve in time. This analysis has been extended from the linear regime to the very problematic nonlinear regime. More precisely, our code describes correctly (§ 4.1) the δ and v evolution in those regions where very steep spatial gradients and very fast temporal changes appear, that is, where caustics begin to develop. Our code has proved to be able to treat initial discontinuous density profiles, giving excellent results (§ 4.2). Other numerical methods fail in those cases in which our code has succeeded; this is not surprising since our code is based on an algorithm specifically designed for solving strong discontinuities. Numerical artifacts (artificial viscosity or other unphysical forces), which are alien to the real physical problem, are not used. The spatial grid is not homogeneous; it has had to be refined in the zones at the neighborhood of the caustic formation. The time step is not constant and it has been chosen in order to resolve the inhomogeneity according to its rate of evolution, i.e., it decreases when the evolution is faster.

The inhomogeneities have been described with the set of equations (5)–(7) proposed by Peebles (1980), and discussed in § 2.2. Its use is familiar in N-body simulations and, in general, in studies of structure formation inside big boxes having a linear size of $\sim 10^2$ Mpc. In the 1D case, the

equations to solve are hyperbolic scalar equations of conservation laws coupled by the source terms. These equations can be solved by using Godunov-type methods.

The goodness of our code depends, crucially, on its generalization possibilities. The goal would be to extend it to be able to evolve three dimensional structures with pressure from general initial conditions of cosmological character. Such code might, eventually, be competitive with the familiar N-body simulations given the fact that pressure could avoid shell crossing, thus allowing the description of the strongly nonlinear regime. Pressure would be introduced as the most natural way of avoiding caustic formation. Indeed, when density grows sufficiently, the baryon component should be a source of pressure which, eventually, could avoid density divergencies.

A 3D extension of our code, including pressure, is feasible theoretically. With pressure, the equations which generalize the system (5)–(7) are a hyperbolic system of conservation laws (with sources). Modern high-resolution shock-capturing schemes have been designed for solving this kind of systems. Nevertheless, a lot of work would be necessary in order to build up a fully 3D code and solve some of the technical details: grid, computational costs, memory capacity, visualization...

Nowadays we are working in a first step towards the above goal. We will introduce the pressure in the system (5)–(7). An equation of state is necessary in order to close this system. In the near future we are planning to study spherically symmetric clusters with pressure —they are one dimensional models— before attacking multidimensional problems. Results in 3D calculations with pressure could be directly compared with observations of the large scale structure of our Universe.

This work has been supported by the Spanish DGICYT (grants PB91-0648 and PB90-0416). The authors have enjoyed fruitful conversations with J. Mª. Martí. The calculations were carried out in a VAX 6000/410 at the Instituto de Física Corpuscular and in an IBM 30-9021 VF at the Centre de Informàtica de la Universitat de València.

REFERENCES

Bardeen, J.M. 1980, Phys. Rev., D22, 1882
Bardeen, J.M., Steinhardt, P.J., & Turner, M.S. 1983, Phys. Rev., D28, 679
Bertschinger, E. 1991, in New Insights into the Universe, eds. V.J. Martínez, M. Portilla & D. Sáez, (Springer-Verlag)
Brandenberger, F.H. 1985, Rev. Mod. Phys., 57, 1
Courant, R., Friedrichs, K.O., & Lewy, H. 1928, Math. Ann., 100, 32
Doroshkevich, A., Ryaben'kii, V., & Shandarin, S.F. 1973, Afz., 9, 144
Doroshkevich, A., & Shandarin, S.F. 1973, Afz., 9, 332
Ellis, G.F.R., & Bruni, M. 1989, Phys. Rev., D40, 1804
Font, J.A., Martí, J.Mª., Ibáñez, J.Mª., & Miralles, J.A. 1993, Comput. Phys. Comm., 75, 31
Fryxell, B.A., Müller, E., & Arnett, W.D. 1990, in Numerical Methods in Astrophysics, ed. P.R. Woodward (Academic Press)
Godunov, S.K. 1959, Matematicheskii Sbornik., 47, 271
Gurbatov, S., Saichev, A., & Shandarin, S.F. 1989, MNRAS, 236, 385
Kofman, L.A., & Linde, A.D. 1987, Nucl. Phys., B298, 555
Lax, P. 1973, in Regional Conference Series Lectures in Applied Math., SIAM (Philadelphia)
Martí, J.Mª. 1991, Ph.D. Thesis, University of Valencia
Martí, J.Mª., Ibáñez, J.Mª., Colomer, F., & Miralles, J.A. 1990, Anales de Física, A86, 47
Martí, J.Mª., Ibáñez, J.Mª., & Miralles, J.A. 1990, A&A, 235, 535
_____. 1991, Phys. Rev., D43, 3794
Matarrese, S., Lucchin, F., Moscardini, L., & Sáez, D. 1992, MNRAS, 259, 437
Matarrese, S., Pantano, O., & Sáez, D. 1993, Phys. Rev., D47, 1311
Mukhanov, V.F., Feldman, H.A., & Brandenberger, R.H. 1992, Phys. Rep., 215, 203
Noh, W.F. 1987, J. Comp. Phys., 72, 78
Oleinik, O.A. 1963, Usp. Mat. Nauk., 12, 3
Peebles, P.J.E. 1980, The Large Scale Structure of the Universe (Princeton, NJ: Princeton University Press)
Roe, P.L. 1981, J. Comp. Phys., 43, 357
Shandarin, S.F., & Zel'dovich, Ya.B. 1989, Rev. Mod. Phys., 61, 185
Van Leer, B. 1979, J. Comp. Phys., 32, 101, Engl. transl., Am. Mat. Soc. Transl. Ser. 2. 26, 95 (1963)
Von Neumann, J., & Richtmyer, R. 1950, J. Appl. Phys., 21, 232
Zel'dovich, Ya.B. 1970, A&A, 5, 84

José Mª. Ibáñez, Vicent Quilis, and D. Sáez: Departamento de Física Teórica, Universidad de Valencia, 46100 Burjassot, Valencia, Spain.